Kinematic Analysis and Stiffness Mapping of Wire-Actuated Parallel Manipulators

with a Rigid Branch

Sureyya Sahin and Leila Notash

Department of Mechanical Engineering
Queen's University
Kingston, Ontario, K7L 3N6
Canada

Abstract: Wire-actuated parallel robots are used for their compactness, high speed and loading capacity. However, establishing the required stiffness in a wire-actuated parallel manipulator could be a problem because of the elastic behaviour of wires. In this article, kinematic and stiffness analyses of wire-actuated parallel manipulators are investigated. An inverse kinematic formulation is given for wire-actuated parallel manipulators with a rigid branch acting on the end effector, and the stiffness matrix of the manipulators are formulated using the result of the inverse kinematics. Then, inverse kinematics and stiffness analysis of a 4 degrees of freedom wire-actuated parallel manipulator is performed as a case study.

1 Introduction

Although the serial mechanisms preserve good obstacle avoidance characteristics and have large workspace, their poor load carrying capacities lead to the usage of closed loop mechanisms, which generally show better weight/load carrying capacities or stiffness characteristics. The stiffness of the closed loop mechanisms is important to investigate their loading capabilities, as well as their deflections due to interaction with their environment.

The stiffness analysis relates the stiffness of the manipulator (caused by elastic components such as links, driving components, etc.) to the end effector stiffness. Simple linear or torsional springs can be used to model the stiffness of the elastic components used in the manipulator. There are various studies on stiffness analysis of manipulators in the literature, and most of these studies consider the actuated joints as the major source of stiffness. Gosselin [3] formulated the stiffness of parallel manipulators under certain assumptions, which resulted in a symmetric stiffness matrix. He used eigenvalue decomposition to investigate the stiffness properties of the parallel manipulator. Griffis and Duffy [4] formulated the stiffness of a parallel mechanism by taking into account the geometric deflection due to the external loading of the manipulator. They used screw theory to formulate the stiffness matrix, and found an asymmetric stiffness matrix. They formulated the stiffness of a Gough-Stewart platform type of a manipulator, which can also be used as a model of a remote center of compliance device. Zefran and Kumar [5] used Lie Algebra and Energy approach to formulate an asymmetric stiffness matrix of closed loop manipulators. They also discussed the cause of the symmetry and asymmetry in the stiffness matrix and concluded that they are due to the layout and geometrical constraints of

the closed loop manipulators. Svinin et al. [6] performed a static force analysis of the general Gough-Stewart type manipulators. They obtained the stiffness matrix by considering the infinitesimal displacement of the manipulators, and related the forces and infinitesimal displacements via the stiffness matrix.

Another factor, which affects the stiffness of the manipulators, is the internal forces, which could act against each other due to the constraints in the closed loop mechanisms [7]. The effects of internal forces can be quite significant depending on the configuration of the manipulator, e.g., if there is redundancy, or the type of the actuator used [8]. Yi and Freeman [9] derived a general formulation of stiffness analysis of closed loop manipulators. They used a dynamical analysis and considered static equilibrium by taking the acceleration terms as zero to obtain the stiffness matrix. They also discussed the cause of the asymmetry in the stiffness matrix, and concluded that the asymmetry is due to geometrical constraints of the manipulator. The stiffness matrix obtained can be used in stability and feedback control of closed loop manipulators.

Wire-actuated parallel manipulators have also been considered in the literature due to their advantages of being lightweight and low cost. One of the main problems of using wires in manipulators is their elastic behaviour. Wires can be used only when they are in tension. Also, establishing the stiffness of the wires is another problem. In Robocrane [10], gravity was used to establish the tension in the wires; therefore the manipulator was able to work only in the presence of gravity forces. Landsberger and Sheridan [11] used wires instead of the legs in a Gough-Stewart type of a manipulator. They designed an additional telescoping rigid branch to maintain the tension in the wires. Kawamura et al. [12] used seven wires for a 6 degrees of freedom manipulator. One of the wires was redundantly used to maintain the tension in the wires. Force closure of wires was considered in the design of the manipulator. A control system with force feedback was employed to guarantee the stiffness of the manipulator.

In this paper kinematic and stiffness of the wire-actuated closed loop manipulators with a rigid branch acting on the end effector are investigated. The main elastic components of the manipulators are the wires and the actuated joints, which are modeled as simple springs. An inverse kinematics solution of the manipulators is given. The principle of virtual work is employed to find the stiffness matrix of the manipulators. The stiffness matrix obtained is symmetric, because the asymmetric effects and the internal forces in the manipulators are neglected. The resultant matrix would be used in inspecting the stiffness characteristics of the manipulators. Stiffness mapping of a 4 degrees of freedom wire-actuated parallel manipulator is obtained to illustrate its stiffness characteristics.

2 Theoretical Background

In this section, the kinematics of wire-actuated manipulators with one rigid branch, acting on the mobile platform, and several actuated wires (branches) is considered. The general configuration of a parallel manipulator with a rigid branch and several active wires is shown in Figure 1. The wires are connected to the ground at points A_i and to the mobile platform at points B_i. The rigid branch consists of links and joints, where the joints are shown as squares in Figure 1.

Some assumptions are made in the configuration of the wires. It is assumed that the necessary tension is established in the wires, and the weights of the wires are neglected so that they preserve the line geometry. As a

result of these assumptions, the wires can be modeled as linkages with a spherical, prismatic and spherical joint combination [13].

For the kinematic analyses of the manipulator, several reference frames are defined, including the base reference frame (frame *0*) with an origin at the centroid of the base platform, and the mobile platform frame (frame *p*) with an origin at the centroid of the mobile platform.

The finite and differential forward and inverse kinematics of the rigid branch are investigated in Section 2.1. Section 2.2 is related to the inverse kinematics of the wires. In Section 2.3, the inverse Jacobian matrix of the parallel manipulator is derived, and a brief explanation on the stiffness matrix is provided.
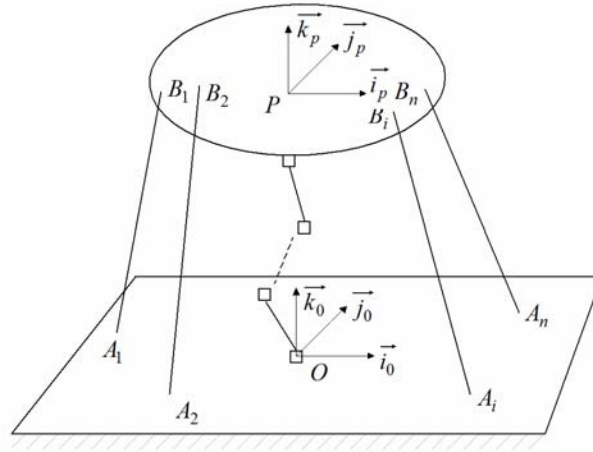

Figure 1 Configuration of a wire actuated parallel robot with a rigid branch.

2.1 Kinematics of the rigid branch

Forward kinematics: For a given configuration of the rigid branch with prismatic or revolute joints, Denavit-Hartenberg convention can be used to attach coordinate frames on the links, and to define the link and joint parameters. Homogeneous transformation matrices can be used to find the position and orientation of the mobile platform in terms of joint variables. The homogeneous transformation matrix relating frame *i* to *i*-1 can be written as:

$$A_{(i-1,i)} = \begin{bmatrix} c\theta_i & -c\alpha_i s\theta_i & s\alpha_i s\theta_i & a_i c\theta_i \\ s\theta_i & c\alpha_i c\theta_i & -s\alpha_i c\theta_i & a_i s\theta_i \\ 0 & s\alpha_i & c\alpha_i & d_i \\ 0 & 0 & 0 & 1 \end{bmatrix} \quad (1)$$

In equation (1), *c* and *s* represent the cosine and sine functions, θ_i is the rotation angle and it is the joint variable for a revolute joint. The joint offset is given by d_i which is the joint variable for a prismatic joint, the twist angle is denoted by α_i, and the link length is represented by a_i. $A_{(i-1,i)}$ is the homogenous transformation matrix between link (*i*-1) and link *i*. The homogenous transformation matrix can be partitioned as follows:

$$A_{(i-1,i)} = \begin{bmatrix} R_{(i-1,i)} & p_{(i-1,i)} \\ 0 \quad 0 \quad 0 & 1 \end{bmatrix} \quad (2)$$

where $\boldsymbol{R}_{(i-1,i)}$ is the 3×3 rotation matrix from link i-1 to link i, and $\boldsymbol{p}_{(i-1,i)}$ is the position of the ith coordinate frame with respect to $(i-1)^{th}$ coordinate frame. For f coordinate frames attached to the rigid branch of the robot, the homogenous transformation matrix between the 0th frame and the platform frame can be calculated by:

$$\boldsymbol{A}_{(0,p)} = \boldsymbol{A}_{(0,f)} = \boldsymbol{A}_{(0,1)} \boldsymbol{A}_{(1,2)} \dots \boldsymbol{A}_{(f-1,f)} \tag{3}$$

Then the position and orientation of the mobile platform can be obtained by extracting the submatrices given by equation (2).

Inverse kinematics: In the inverse kinematics of the rigid branch, for a given position and orientation of the mobile platform, it is desired to find the joint variables. The known position and orientation of the platform can be equated to the results of equation (3) and solved for the joint variables.

Velocity analysis: The Jacobian matrix of the rigid branch, $\boldsymbol{J}_b$, can be derived by using the position, $\boldsymbol{p}_{(i-1,i)}$, and orientation, $\boldsymbol{R}_{(i-1,i)}$, entities of equation (2). The conventional formulations for calculating the Jacobian matrix, defined in the literature, can be used for deriving the velocity relation. Then,

$$\boldsymbol{v} = \boldsymbol{J}_b \dot{\boldsymbol{q}}_b \tag{4}$$

where $\boldsymbol{v}$ is the mobile platform velocity (angular velocity of the platform and linear velocity of the origin of mobile platform frame), and $\boldsymbol{q}_b$ is the vector of joint variables for the rigid branch. The inverse velocity analysis of the rigid branch will be as follows

$$\dot{\boldsymbol{q}}_b = \boldsymbol{J}_b^{-1} \boldsymbol{v} \tag{5}$$

In general not all of the joints of the rigid branch will be actuated, i.e., m out of n joints ($m \leq n$) will be actuated. Equations (4) and (5) include the velocities of both active and passive joints of the rigid branch. From equation (5) rows, which contain the actuated joint velocity variables, can be extracted and used in the inverse Jacobian of the parallel manipulator [14].

2.2 Inverse kinematic analysis of the wires

Using loop closure equations, the inverse kinematics of the wires can be solved. It is assumed that the wires remain in tension all the time. A loop closure equation can be written for the ith wire as:

$$\overline{OA_i} + \overline{A_i B_i} = \overline{OP} + \overline{PB_i} \tag{6}$$

If the wire length vector is denoted as $\boldsymbol{l}_i = \overline{A_i B_i}$, then the ith wire length vector can be calculated as:

$$\boldsymbol{l}_i = \overline{OP} + \boldsymbol{R}_{(0,p)} {}^{P}\overline{PB_i} - \overline{OA_i} \tag{7}$$

The Euclidean norm of equation (7) can be taken to find the wire length.

The velocity of wire lengths can be found by taking the time derivative of equation (7) as follows:

$$\dot{\boldsymbol{l}}_i = \overline{\dot{OP}} + \dot{\boldsymbol{R}}_{(0,p)} {}^{P}\overline{PB_i} \tag{8}$$

The Euclidean norm of equation (8) will give the magnitude of the rate of change of the ith wire length. Hence, an equation, which relates the mobile platform velocities to the magnitude of the wire velocities, can be found. Equation (8) will be used to obtain the Jacobian of the parallel manipulator.

2.3 Stiffness analysis of the manipulator

The stiffness of the parallel manipulator can be investigated using the Jacobian of the manipulator. Since the manipulator consists of m actuated joints on the rigid branch and n wires, the following relation can be obtained between the mobile platform velocity and the joint/wire velocity.

$$\begin{bmatrix} \dot{q}_1 \\ \vdots \\ \dot{q}_m \\ \|\dot{l}_1\| \\ \vdots \\ \|\dot{l}_n\| \end{bmatrix} = J^{-1}v \tag{9}$$

An infinitesimal displacement of the actuators (active joints and wires) could be related to the infinitesimal displacement of the mobile platform as:

$$\Delta q = J^{-1}\Delta x \tag{10}$$

Using the work-energy method, the following relation can be obtained between the actuator forces/torques, denoted by τ, and mobile platform forces and moments, denoted by F:

$$F = J^{-T}\tau \tag{11}$$

Under the assumption that there is an infinitesimal displacement of actuators, the following relation between the actuator forces and the displacements hold:

$$\tau = K_a \Delta q \tag{12}$$

K_a is a diagonal matrix whose element k_i denote the stiffness of the ith-actuated quantity (joint or wire). Using equations (10) through (12), the relation between the mobile platform force (wrench) applied by its environment and an infinitesimal displacement of the mobile platform can be obtained:

$$F = K_{mp}\Delta x \tag{13}$$

$$K_{mp} = J^{-T}K_a J^{-1} \tag{14}$$

where K_{mp} is the stiffness matrix of the manipulator, and K_a is the stiffness of the actuated joints/wires. This matrix will be used to map the stiffness of the manipulator to the Cartesian space.
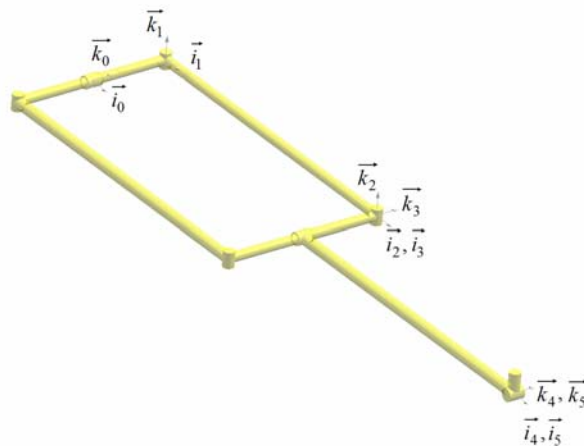
3. Example Manipulator

The manipulator considered in this section has four degrees of freedom, and includes three wires and a rigid branch acting on the centre of the mobile platform [15]. The branch consists of a parallelogram mechanism, and

a link for connecting the mobile platform to the parallelogram mechanism. The two joints closest to the base, namely the ones at the origins of coordinate frames O_0 and O_1, are actuated. Additionally, three wires attached to points A_i on the base, and points B_i on the moving links, are used to control the mobile platform, as shown in Figure 2.
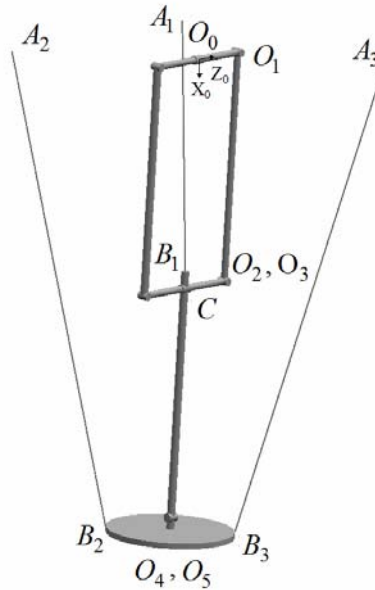
Figure 2 Example wire-actuated parallel manipulator.

Figure 3 Zero configuration of the rigid branch of the example manipulator.

A zero configuration of the rigid branch and its Denavit-Hartenberg parameters are given in Figure 3 and Table 1, respectively.

Table 1 Denavit-Hartenberg parameters of example manipulator.

Link	θ_i	d_i	a_i	α_i
1	θ_1	d_1	0	$\pi/2$
2	θ_2	0	a_2	0
3	θ_3	0	0	$-\pi/2$
4	θ_4	$-d_4$	a_4	0
5	θ_5	0	0	0

3.1 Inverse kinematics of the rigid branch

Using the methodology discussed in Section 2.1, the inverse kinematics of the rigid branch can be performed. The position of the end effector of the manipulator can be written as:

$$\boldsymbol{p}_{(0,5)} = \begin{bmatrix} a_2 c\theta_2 c\theta_1 + a_4 c\theta_{14} \\ a_2 c\theta_2 s\theta_1 + a_4 s\theta_{14} \\ a_2 s\theta_2 + d_1 - d_4 \end{bmatrix} \tag{15}$$

The orientation of the manipulator can be given as a rotation about the third axis by an angle $\theta_{145} = \theta_1 + \theta_4 + \theta_5$. The inverse kinematics of the rigid branch can be obtained for a given position and orientation of the end effector as:

$$\theta_1 = 2 a \tan 2 ((-r_1^* + \sqrt{(r_1^*)^2 + (r_2^*)^2 - (a_4 s\theta_4)^2}), (r_2^* + a_4 s\theta_4)) \tag{16}$$

$$\theta_2 = a\tan 2(\frac{r_3^*}{a_2}, \sqrt{1 - (\frac{r_3^*}{a_2})^2}) \tag{17}$$

$$\theta_3 = -\theta_2 \tag{18}$$

$$\theta_4 = \pm a\cos\left(\frac{(r_1^*)^2 + (r_2^*)^2 - a_4^2 - (a_2 c\theta_2)^2}{2a_2 a_4 c\theta_2} \right) \tag{19}$$

$$\theta_5 = \alpha - \theta_1 - \theta_4 \tag{20}$$

where $r^* = \begin{bmatrix} r_1^* & r_2^* & r_3^* \end{bmatrix}^T = \boldsymbol{p}_{(0,5)} - [0 \ 0 \ d_1 - d_4]^T$, and α is the pitch angle of the end effector. Also, due to limitations of the manipulator, the range of θ_2 is considered to be between $-\pi/2$ and $\pi/2$. Both solutions for θ_4 are acceptable since they are in the working range.

Completing the position analysis, the Jacobian of the rigid branch, denoted by J_b, can be found as:

$$J_b = \begin{bmatrix} -a_2 c\theta_2 s\theta_1 - a_4 s\theta_{14} & -a_2 c\theta_1 s\theta_2 & -a_4 s\theta_{14} & 0 \\ a_2 c\theta_2 c\theta_1 + a_4 c\theta_{14} & -a_2 s\theta_1 s\theta_2 & a_4 c\theta_{14} & 0 \\ 0 & a_2 c\theta_2 & 0 & 0 \\ 1 & 0 & 1 & 1 \end{bmatrix} \tag{21}$$

where $\theta_{14} = \theta_1 + \theta_4$.

The inverse Jacobian matrix of the branch can be calculated by taking the inverse of J_b. Then the first two rows of the resultant matrix equation, which represent the relation between the actuated joint variables of the branch and the mobile platform velocity, can be extracted and used in formulating the Jacobian of the parallel manipulator.

3.2 Kinematics of the wires

The inverse kinematics of the wires can be performed in a similar manner as explained in Section 2.2. The loop closure equations for the wires can be written as:

$$\overline{O_0A_1} + \overline{A_1B_1} = \overline{O_0O_3} + \overline{O_3C} + \overline{CB_1} \tag{22}$$

$$\overline{O_0A_2} + \overline{A_2B_2} = \overline{O_0O_5} + \overline{O_5B_2} \tag{23}$$

$$\overline{O_0A_3} + \overline{A_3B_3} = \overline{O_0O_5} + \overline{O_5B_3} \tag{24}$$

Then, the wire length vectors in the base reference frame can be found by arranging equations (22) through (24) as follows

$$l_1 = (a_2 c\theta_2 c\theta_1 - a_5 c\theta_{14})i_0 + (a_2 s\theta_2 s\theta_1 - a_5 s\theta_{14})j_0 + (d_1 - d_4)k_0 - \overline{O_0A_1} \tag{25}$$

$$l_2 = p_{(0,5)} + R_{(0,5)}\overline{O_5B_2} - \overline{O_0A_2} \tag{26}$$

$$l_3 = p_{(0,5)} + R_{(0,5)}\overline{O_5B_3} - \overline{O_0A_3} \tag{27}$$

where i_0, j_0 and k_0 are the unit vectors of the base reference frame, and $a_5 = \left\| \overline{CB_1} \right\|$.

Equations (25) through (27) can be used to find the wire displacements and the remaining three rows of the Jacobian matrix of the parallel manipulator. The velocity relations that can be used in finding the Jacobian are:

$$\dot{l}_1 = v - (\dot{\theta}_1 + \dot{\theta}_4)R_{(0,4)}\tilde{k}_0((a_4 + a_5)i_0) \tag{28}$$

$$\dot{l}_2 = v + \dot{\alpha} R_{(0,5)}\tilde{k}_0 \overline{O_5B_2} \tag{29}$$

$$\dot{l}_3 = v + \dot{\alpha} R_{(0,5)}\tilde{k}_0 \overline{O_5B_3} \tag{30}$$

In the above set of equations, $\dot{\alpha}$ is the angular velocity of the platform in the pitch direction, and (~) is the skew symmetric matrix operator for taking the cross product of two vectors.

Then the Jacobian matrix can be written as:

$$\begin{bmatrix} \dot{\theta}_1 \\ \dot{\theta}_2 \\ \|\dot{l}_1\| \\ \|\dot{l}_2\| \\ \|\dot{l}_3\| \end{bmatrix} = J^{-1}\begin{bmatrix} v \\ \dot{\alpha} \end{bmatrix} \tag{31}$$

where

$$J^{-1} = \begin{bmatrix} \dfrac{c\theta_{14}}{a_2 c\theta_2 s\theta_4} & \dfrac{s\theta_{14}}{a_2 c\theta_2 s\theta_4} & \dfrac{s\theta_2(s\theta_{14}c\theta_{14}+s\theta_1 c\theta_1)}{a_2 c^2\theta_2(c^2\theta_{14}-c^2\theta_1)} & 0 \\ 0 \quad 0 & \dfrac{1}{a_2 c\theta_2} & 0 \\ n_1^T - n_1^T\left[(R^{(0,4)}\widetilde{k}_0(a_4+a_5)i_0)t^T\right] & & 0 \\ n_2^T & & n_2^T R^{(0,5)}\widetilde{k}_0\overline{O_5 B_2} \\ n_3^T & & n_3^T R^{(0,5)}\widetilde{k}_0\overline{O_5 B_3} \end{bmatrix} \tag{32}$$

The first two rows of J^{-1} is obtained by inverting equation (21) and extracting the first two rows. The last three rows are obtained by using the equations (28) through (30). The term t^T is obtained by eliminating $\dot{\theta}_1$ and $\dot{\theta}_4$ which appear in equation (28) and is found as:

$$t^T = \begin{bmatrix} \dfrac{-c\theta_1}{a_4 s\theta_4} & \dfrac{-s\theta_1}{a_4 s\theta_4} & \dfrac{-s\theta_2}{a_4 s\theta_4 c\theta_2} \end{bmatrix} \tag{33}$$

The n_i terms represent the unit vectors acting along the direction of the wires, and calculated by using equations (25) through (27).

4. Stiffness Mapping

After completing the Jacobian analysis of the system, the stiffness matrix can be calculated using the discussion of Section 2.3. Equations (14) and (32) can be used with the stiffness matrix of the actuated joints and wires of the manipulator, which is:

$$K_a = \begin{bmatrix} K_\theta & 0 \\ 0 & K_l \end{bmatrix} \tag{34}$$

where K_θ is a diagonal matrix which is composed of the stiffness of actuated joints in the rigid branch, and K_l is a diagonal matrix which includes the stiffness of the wires.

A computer simulation is performed to obtain some preliminary results of the stiffness of the manipulator. Regions in the workspace are considered for the simulation and eigenvalue decomposition is used to obtain the stiffness components of the manipulator in X_0, Y_0 and Z_0 directions, while the orientation is kept constant. The results are shown in Figures (4) through (6), symmetry of the manipulator can be observed from these plots.
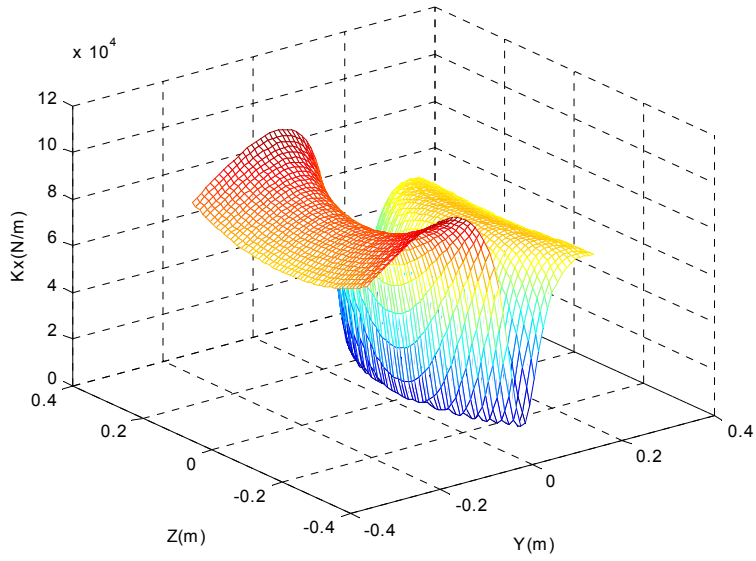
Figure 4 Stiffness of the example manipulator in X_0 direction.
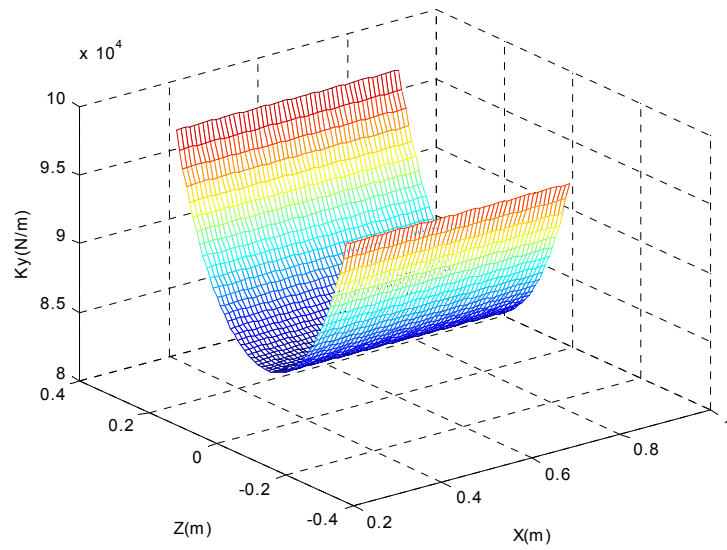
Figure 5 Stiffness of the example manipulator in Y_0 direction.
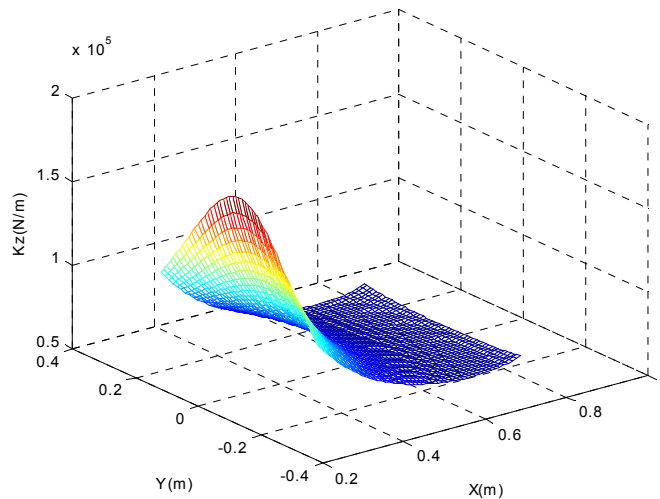
Figure 6 Stiffness of the example manipulator in Z_0 direction.

5. Concluding Remarks

In this article, the kinematic modelling and stiffness analysis of wire-actuated parallel manipulators were considered.

A class of wire-actuated parallel manipulators with one rigid branch and several wires was presented. The kinematic analysis of this class of manipulators was performed. The derivation of inverse Jacobian matrix and the stiffness analysis were discussed. The resultant formulation was applied to a 4 degrees of freedom parallel wire-actuated manipulator. Stiffness mapping of the manipulator was plotted in certain regions of the workspace, in which the symmetry of the manipulator was observed due to the formulas used for obtaining the stiffness matrix.

A detailed stiffness analysis, which contains the effects of internal forces and external loading as discussed in the literature, is currently under investigation.

References

1. Tsai, L.W., Robot Analysis, The Mechanics of Serial and Parallel Manipulator, John Wiley and Sons Inc., 1999

2. Merlet, J.-P., Parallel Robot, Kluwer Academic Publishers, 2000

3. Gosselin, C., Stiffness Mapping for Parallel Manipulators, IEEE Trans. Robotics and Automation, 6(3):377-382, 1990

4. Griffis M., and Duffy J., Kinestatic Control: A Novel Theory for Simultaneously Regulating Force and Displacement, Trans. ASME Mechanical Design, 113:508-515, 1991

5. Zefran, M., and Kumar, V., Affine Connections for the Cartesian Stiffness Matrix, Proc. IEEE Int. Conference on Robotics and Automation, pp1376-1381, 1997

6. Svinin, M. M., Hosoe, S., and Uchiyama, M., On the Stiffness and Stability of Gough-Stewart Platform, Proc. IEEE Int. Conference on Robotics and Automation, pp. 3268-3273, 2001

7. Adli, M., A., Nagai, K., Miyata, K., and Hanafusa, H., Apparent Structural Stiffness of Closed Mechanisms under the effect of Internal Forces During Dynamic Motion, IEEE Int. Workshop on Intelligent Robots and Systems, pp. 773-778, 1991

8. Chakarov, D., Study of the passive compliance of parallel manipulators, Mechanism and Machine Theory, 34(3):373-389, 1999

9. Yi B., and Freeman R., Geometric Analysis of Antagonistic Stiffness in Redundantly Actuated Parallel Mechanisms, J. Robotic Systems, 10(5):581-603,1992

10. Albus J., Bostelman R., and Dagalakis N., The NIST SPIDER, a Robot Crane, Journal of Research of the National Institute of Standards and Technology, 97(3):373-385, 1992

11. Landsberger, S.E., and Sheridan T.B., A Minimal Minimal Linkage: The Tension Compression Parallel Link Manipulator, Robotics, Mechatronics and Manufacturing Systems, pp. 81-88, 1993

12. Kawamura, S., Kino, H., and Won, C., High Speed Manipulation by Using Parallel Wire-Driven Robots, Robotica, Vol. 18, pp. 13-21, 2000

13. Ming, H., and Higuchi, T., Study on Multiple Degree of Freedom Positioning Mechanism Using Wires (Part 1), International J. the Japan Society for Precision Eng., 28(2): 131-138, 1994

14. Kumar V., and Gardner J. F., Kinematics of Redundantly Actuated Closed Chains, IEEE Trans. Robotics and Automation, 6(2): 269-274, 1990

15. Mroz, G., and Notash, L., Design and Prototype of a Parallel Wire-Actuated Manipulator, to appear in Proc. 11th World Congress on Mechanism and Machine Science, 2004